

Channel Model for Low Voltage Three-Core Power Line Communication

YIHE GUO¹, ZHE YANG¹, RAN HUO², AND ZHIYUAN XIE¹

¹School of Electrical and Electronic Engineering, North China Electric Power University, Baoding 071003, China

²State Grid Information and Telecommunication Group Company Ltd., Beijing 100000, China

Corresponding author: Yihe Guo (yihe_guo@163.com)

This work was supported in part by the Science and Technology Program of Hebei Province under Grant 17211704D, and in part by the Fundamental Research Funds for the Central Universities under Grant 2015MS97.

ABSTRACT The influences of proximity effect and complex dielectric permittivity on per-unit-length parameter matrices of three-core power line are analyzed. Based on the symmetrical structure of three-core cable, the per-unit-length parameter matrices are decomposed into common mode and differential mode parameters by phase-mode transformation. Taking the electromagnetic simulation results of finite element method as the initial values, a method of correcting per-unit-length parameters based on open-circuit impedance measurement in mode domain is proposed. Based on the theory of multi-conductor transmission line, the channel model of three-core power line in the frequency range from 30 kHz up to 15 MHz is established. The test results under the branch network show that the channel model has high accuracy, and the influence of the network structure on the impedance and transmission characteristics is further analyzed. The model can accurately take into account the coupling effect between multiple-input multiple-output channels.

INDEX TERMS Power line communication, multi-conductor transmission line, phase-mode transformation, per-unit-length parameter matrices, multiple-input multiple-output.


I. INTRODUCTION

power line communications (PLC) have been applied as a data transfer method in both public electricity distribution networks and indoor distribution networks. In the field of automatic meter reading (AMR), low voltage narrowband PLC (in the frequency range from 40 kHz to 500 kHz) accounts for more than 80% of various communication methods in China. Broadband PLC (in the frequency range from 700 kHz to 12 MHz) has been widely used in recent years also. The frequency range studied in this paper is from 30kHz to 15 MHz, which covers the narrowband and broadband applications for AMR in China.

For multi-core power cables, multiple-input multiple-output (MIMO) communication can be used to further increase channel capacity. In the field of MIMO PLC, a large amount of measurements and research has been carried out, and some statistical channel models have been proposed based on the top-down method [1]–[4]. The bottom-up model can be used to calculate transmission and impedance characteristics and analyze the coupling effect between core wires. There are many difficulties in the accurate acquisition of

the per-unit-length parameters matrices of multi-core power cables. The transmission characteristics of two three-core cables have been analyzed, and the per-unit-length parameters matrices have been calculated by an approximate formula [5]. Because the effect of proximity effect and insulation medium cannot be accurately calculated, the error between the calculation and measurement is large. In [6], the symmetrical three-core cable has been simplified into a two-wire cable, which makes it impossible to study the coupling effect between the core wires. For the shielded three-core XLPE cable, an approximate calculation method has been proposed in [7]. Based on the phase-mode transformation method, the propagation speed and the characteristic impedance are calculated and measured. Because the dielectric constant of insulation medium is considered as a constant, the error between calculation and measurement is obvious. For the busbar energy distribution system with a length of 3m, Zeynep Hasirci uses a nonlinear optimization algorithm to determine the per-unit-length parameters [8], [9]. The algorithm takes the minimum error of all S parameters as the optimization target, which leads to high computational complexity.

This paper proposes a new modeling method. Since the permittivity of the insulation medium is difficult to measure directly, the initial values of per-unit-length parameters are

The associate editor coordinating the review of this manuscript and approving it for publication was Matti Hämäläinen .

obtained by electromagnetic simulation based on the finite element method, and then the errors are corrected by the measurement results of open-circuit impedance. Because there are many parameters to be solved in multi-core cables and each parameter will affect the channel characteristics in various ways, this paper proposes a parameter correction methods in mode domain.

II. MODELING METHOD OF POWER LINE

A. MULTI-CONDUCTOR TRANSMISSION LINE MODEL

The BVVB three-core cable under study in this paper, as shown in Fig. 1, is the typical single-phase electric wires in China.

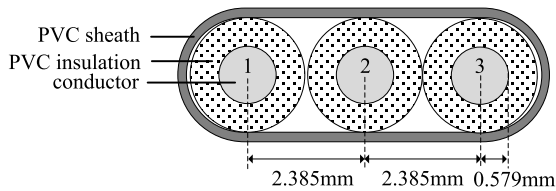


FIGURE 1. Cross section of three-core power cable.

The three-core wires are sequentially labeled as 1, 2, and 3 from left to right. To study the propagation characteristics of high-frequency carrier signals through three-core power line, multi-conductor transmission line (MTL) equations are used. If the per-unit-length parameter matrices are \mathbf{R}_0 , \mathbf{L}_0 , \mathbf{G}_0 and \mathbf{C}_0 and the angular frequency of signal is ω , the series impedance matrix is given by $\mathbf{Z}_0 = \mathbf{R}_0 + j\omega\mathbf{L}_0$, and the parallel admittance matrix is given by $\mathbf{Y}_0 = \mathbf{G}_0 + j\omega\mathbf{C}_0$. The MTL equations can be described as [10]

$$\begin{cases} \frac{d^2}{dx^2} \mathbf{U}(x) = \mathbf{Z}_0 \mathbf{Y}_0 \mathbf{U}(x) \\ \frac{d^2}{dx^2} \mathbf{I}(x) = \mathbf{Y}_0 \mathbf{Z}_0 \mathbf{I}(x) \end{cases} \quad (1)$$

where $\mathbf{U}(x)$ and $\mathbf{I}(x)$ are column vectors of voltages and currents, respectively. Since $\mathbf{Z}_0 \mathbf{Y}_0$ and $\mathbf{Y}_0 \mathbf{Z}_0$ are not diagonal matrices, the voltage and current of each conductor interact with each other, and the transmission line equation cannot be solved directly. The transformation matrix \mathbf{T}_V or \mathbf{T}_I is introduced to decouple the equation. Since both \mathbf{Z}_0 and \mathbf{Y}_0 are symmetric matrices it can be proved that $\mathbf{T}_I^T = \mathbf{T}_V^{-1}$, and the two transformation matrices satisfy

$$\mathbf{T}_V^{-1} \mathbf{Z}_0 \mathbf{Y}_0 \mathbf{T}_V = \mathbf{T}_I^{-1} \mathbf{Y}_0 \mathbf{Z}_0 \mathbf{T}_I = \begin{bmatrix} \gamma_1^2 & 0 \\ 0 & \gamma_2^2 \end{bmatrix} \quad (2)$$

where γ_i^2 ($i = 1, 2$) is the eigenvalue of $\mathbf{Z}_0 \mathbf{Y}_0$ and $\mathbf{Y}_0 \mathbf{Z}_0$. A uniform transmission line can be described by the chain-parameter matrix as [11]

$$\begin{bmatrix} \mathbf{U}(l) \\ \mathbf{I}(l) \end{bmatrix} = \begin{bmatrix} \mathbf{A}_{11} & \mathbf{A}_{12} \\ \mathbf{A}_{21} & \mathbf{A}_{22} \end{bmatrix} \begin{bmatrix} \mathbf{U}(0) \\ \mathbf{I}(0) \end{bmatrix} \quad (3)$$

where $\mathbf{U}(l)$ and $\mathbf{I}(l)$ are the voltage and current vectors at the load end, $\mathbf{U}(0)$ and $\mathbf{I}(0)$ are the voltage and current vectors

at the source end. The four chain parameters are [12]

$$\begin{cases} \mathbf{A}_{11} = \frac{1}{2} \mathbf{Y}_0^{-1} \mathbf{T} (e^{\gamma l} + e^{-\gamma l}) \mathbf{T}^{-1} \mathbf{Y}_0 \\ \mathbf{A}_{12} = -\frac{1}{2} \mathbf{Y}_0^{-1} \mathbf{T} \boldsymbol{\gamma} (e^{\gamma l} - e^{-\gamma l}) \mathbf{T}^{-1} \\ \mathbf{A}_{21} = -\frac{1}{2} \mathbf{T} (e^{\gamma l} - e^{-\gamma l}) \boldsymbol{\gamma}^{-1} \mathbf{T}^{-1} \mathbf{Y}_0 \\ \mathbf{A}_{22} = \frac{1}{2} \mathbf{T} (e^{\gamma l} + e^{-\gamma l}) \mathbf{T}^{-1} \end{cases} \quad (4)$$

where $\mathbf{T} = \mathbf{T}_I$, $e^{\gamma l} = \begin{bmatrix} e^{\gamma_1 l} & 0 \\ 0 & e^{\gamma_2 l} \end{bmatrix}$.

In order to calculate the terminal voltages and currents, the Norton equivalent is used, which contains the independent current sources \mathbf{I}_s and admittance \mathbf{Y}_s . The load is represented by the admittance \mathbf{Y}_l .

$$\begin{aligned} \mathbf{U}(0) &= (\mathbf{A}_{21} - \mathbf{A}_{22} \mathbf{Y}_s - \mathbf{Y}_l \mathbf{A}_{11} + \mathbf{Y}_l \mathbf{A}_{12} \mathbf{Y}_s)^{-1} \\ &\quad \cdot (\mathbf{Y}_l \mathbf{A}_{12} - \mathbf{A}_{22}) \mathbf{I}_s \\ \mathbf{U}(l) &= \mathbf{A}_{12} \mathbf{I}_s + (\mathbf{A}_{11} - \mathbf{A}_{12} \mathbf{Y}_s) \mathbf{U}(0) \\ \mathbf{I}(0) &= \mathbf{I}_s - \mathbf{Y}_s \mathbf{U}(0) \\ \mathbf{I}(l) &= \mathbf{Y}_l \mathbf{U}(l) \end{aligned} \quad (5)$$

Then, the input impedance and voltage transfer function can be further solved.

B. ANALYSIS OF PER-UNIT-LENGTH PARAMETERS

The per-unit-length parameter matrices are the basis for the calculation of the MTL equations. There are many difficulties in solving the per-unit-length parameters of the power line accurately. The skin effect occurs when high-frequency current flows through the power line. Due to the relatively small wire spacing of the cable, the proximity effect should be also considered carefully [13]. The charge distributions will tend to concentrate on the adjacent surfaces, which increases per-unit-length resistances. When proximity effect is pronounced, the classical calculation formulas would lead to unacceptable errors.

Polyvinyl chloride (PVC) is often used as insulation and sheath for actual low voltage power cables. The permittivity of PVC may be a slight function of frequency. The manufacturer of power cable cannot provide the accurate values of permittivity at high frequency, and there are more than one layer of materials in the cable, which make it impossible to accurately calculate the per-unit-length capacitance and conductance by the formula method. In order to describe these two electrical characteristics of dielectric, the complex permittivity is introduced and defined as [14], [15]

$$\epsilon_r = \epsilon_r' - i\epsilon_r'' \quad (6)$$

where ϵ_r' is the real part of the permittivity which is associated with the capacitance and ϵ_r'' is the imaginary part which is associated with the conductance. In practice, the loss tangent $\tan(\theta)$ is usually used to describe this relationship.

$$\tan(\theta) = \frac{\epsilon_r''}{\epsilon_r'} \quad (7)$$

Compared with the analytical formulas, the per-unit-length parameters, which are extracted by the electromagnetic field simulation tool, have higher precision [16]. However, due to the uncertainty of the complex permittivity, the simulation results of per-unit-length parameters are also inaccurate. For this reason, this paper proposes a method for solving the cable model parameters, which combines electromagnetic field simulation and open-circuit impedance measurement.

III. SOLUTION OF CABLE MODEL

A. PHASE-MODE TRANSFORMATION

If the intermediate core is chosen the reference conductor, the symmetrical three-core cable can be seen as 2 + 1 transmission lines system, as shown in Fig. 1. The per-unit-length parameter matrices are

$$\mathbf{R}_0 = \begin{bmatrix} R_s & R_m \\ R_m & R_s \end{bmatrix} \quad (8)$$

$$\mathbf{L}_0 = \begin{bmatrix} L_s & L_m \\ L_m & L_s \end{bmatrix} \quad (9)$$

$$\mathbf{G}_0 = \begin{bmatrix} G_s & G_m \\ G_m & G_s \end{bmatrix} \quad (10)$$

$$\mathbf{C}_0 = \begin{bmatrix} C_s & C_m \\ C_m & C_s \end{bmatrix} \quad (11)$$

where G_m and C_m are negative. From (8)–(10), there are eight parameters, all of which influence the channel characteristics synthetically. Taking three-core cable used in this paper as an example, each per-unit-length parameter matrix, $\mathbf{Z}_0\mathbf{Y}_0$ and $\mathbf{Y}_0\mathbf{Z}_0$ are all 2×2 matrices. The main diagonal elements are equal, and the off-diagonal elements are also equal. The phase-mode transformation matrix \mathbf{T} is independent of frequency as

$$\mathbf{T} = \mathbf{T}_V = \mathbf{T}_I = \frac{1}{\sqrt{2}} \begin{bmatrix} 1 & 1 \\ -1 & 1 \end{bmatrix} \quad (12)$$

According to (12), the propagation modes are split into two different mode sets, as shown in Fig. 2.

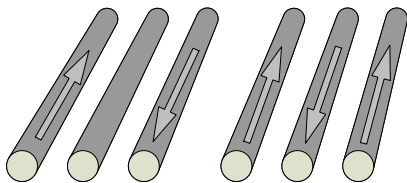


FIGURE 2. Propagation modes of three-core power cable.

Among them, the differential mode (DM) signals, which are equal in magnitude and opposite in direction, propagates along the conductors on left-hand and right-hand sides. The common mode (CM) signals return through the middle reference conductor, and the currents flowing through the two sides are equal in magnitude and in the same direction.

According to (8)–(10), \mathbf{Z}_0 and \mathbf{Y}_0 can be obtained as

$$\mathbf{Z}_0 = \begin{bmatrix} Z_s & Z_m \\ Z_m & Z_s \end{bmatrix} = \begin{bmatrix} R_s & R_m \\ R_m & R_s \end{bmatrix} + \begin{bmatrix} j\omega L_s & j\omega L_m \\ j\omega L_m & j\omega L_s \end{bmatrix} \quad (13)$$

$$\mathbf{Y}_0 = \begin{bmatrix} Y_s & Y_m \\ Y_m & Y_s \end{bmatrix} = \begin{bmatrix} G_s & G_m \\ G_m & G_s \end{bmatrix} + \begin{bmatrix} j\omega C_s & j\omega C_m \\ j\omega C_m & j\omega C_s \end{bmatrix} \quad (14)$$

then

$$\mathbf{T}^{-1}\mathbf{Y}_0\mathbf{Z}_0\mathbf{T} = \begin{bmatrix} (Y_s - Y_m)(Z_s - Z_m) & 0 \\ 0 & (Y_s + Y_m)(Z_s + Z_m) \end{bmatrix} \quad (15)$$

From (2) and (15), the propagation constant of DM is

$$\gamma_1 = \sqrt{[(R_s - R_m) + j\omega(L_s - L_m)] \cdot [(G_s - G_m) + j\omega(C_s - C_m)]} \quad (16)$$

The propagation constant of CM is

$$\gamma_2 = \sqrt{[(R_s + R_m) + j\omega(L_s + L_m)] \cdot [(G_s + G_m) + j\omega(C_s + C_m)]} \quad (17)$$

The characteristic impedance matrix in the mode domain is

$$\mathbf{Z}_{mc} = \begin{bmatrix} \sqrt{\frac{Z_s - Z_m}{Y_s - Y_m}} & 0 \\ 0 & \sqrt{\frac{Z_s + Z_m}{Y_s + Y_m}} \end{bmatrix} \quad (18)$$

From the diagonal elements in (18), the characteristic impedance of DM is

$$Z_1 = \sqrt{\frac{(R_s - R_m) + j\omega(L_s - L_m)}{(G_s - G_m) + j\omega(C_s - C_m)}} \quad (19)$$

The characteristic impedance of CM is

$$Z_2 = \sqrt{\frac{(R_s + R_m) + j\omega(L_s + L_m)}{(G_s + G_m) + j\omega(C_s + C_m)}} \quad (20)$$

Comparing the propagation constants and characteristic impedances from (16)–(20), it can be seen that the four per-unit-length parameters of DM are $R_s - R_m$, $L_s - L_m$, $G_s - G_m$ and $C_s - C_m$ and the four per-unit-length parameters of CM are $R_s + R_m$, $L_s + L_m$, $G_s + G_m$ and $C_s + C_m$. There are two individual two-conductor transmission line systems in the mode domain. By solving the two sets of per-unit-length parameters, the actual per-unit-length parameter matrices can be calculated.

B. PRINCIPLE OF SOLVING PER-UNIT-LENGTH PARAMETERS

According to the cross sections of the three-core cable, all per-unit-length parameter matrices \mathbf{R}_0 , \mathbf{L}_0 , \mathbf{C}_0 and \mathbf{G}_0 are extracted based on the two-dimensional electromagnetic field simulation tool of ANSYS. Through the simple calculation of matrices elements, the initial values of per-unit-length parameters of DM and CM are obtained respectively. Since the per-unit-length resistances and inductances are not affected by insulation materials, the simulation results of \mathbf{R}_0 and \mathbf{L}_0 are accurate, but \mathbf{C}_0 and \mathbf{G}_0 need to be corrected. Without loss

of generality, we assume that $\epsilon'_r = 3$ and $\tan(\theta) = 0$ in the simulation.

By the phase-mode transformation, the impedance and transmission characteristics of the three-core cable in the mode domain are similar to the two-conductor transmission line so that a simple linear correction can be used to increase the model accuracy. In the following, the method of parameter correction is presented based on two-conductor transmission line, which can be applied to both DM and CM.

Assuming that the per-unit-length parameters of the uniform transmission line are R , L , G , and C , the secondary parameters can be further obtained. The propagation constant is

$$\gamma_b = \alpha + j\beta = \sqrt{(R + j\omega L)(G + j\omega C)} \quad (21)$$

where α is the attenuation constant and β is the phase constant. The characteristic impedance is

$$Z_C = \sqrt{\frac{R + j\omega L}{G + j\omega C}} \quad (22)$$

If the load terminal is open-circuited, the input impedance looking into a line with length l_b is

$$Z_{ino} = Z_C \frac{1 + e^{-2\gamma_b l_b}}{1 - e^{-2\gamma_b l_b}} \quad (23)$$

In the frequency range up to 15 MHz, the power line generally meets the low-loss conditions: $R \ll \omega L$ and $G \ll \omega C$. So the approximate expression of (21) and (22) are

$$\gamma_b \approx j\omega\sqrt{LC} \left[1 - j \left(\frac{R}{2\omega L} + \frac{G}{2\omega C} \right) \right] \quad (24)$$

$$Z_C \approx \sqrt{\frac{L}{C}} \quad (25)$$

Substituting (24) and (25) into (23), the input impedance can be simplified as

$$Z_{ino} \approx Z_C \frac{1 + e^{-(R/Z_C + G \cdot Z_C)l_b} e^{-2j\omega\sqrt{LC}l_b}}{1 - e^{-(R/Z_C + G \cdot Z_C)l_b} e^{-2j\omega\sqrt{LC}l_b}} \quad (26)$$

The periodicity of Z_{ino} is the same as the $e^{-2j\omega\sqrt{LC}l_b}$ which is determined by the primary parameters L , C and line length l_b . Using the simulation result of L and the known l_b , the exact per-unit-length capacitance C can be obtained by minimizing the error between measured and the calculated period. The actual capacitance can be written as

$$C_C = m \left(1 + n \frac{f}{f_{end}} \right) C \quad (27)$$

where f is the frequency and f_{end} is the maximum frequency (15 MHz), and m and n are the undetermined coefficients. According to the error of the first few periods, the coefficient m is determined to eliminate the low-frequency error. If the error in the high-frequency range is unacceptable, the coefficient n is determined to meet the accuracy requirements in the entire frequency range.

The magnitude of Z_{ino} is determined by $e^{-(R/Z_C + G \cdot Z_C)l_b}$. As the frequency increases, the magnitude of Z_{ino} decreases. Basically, the per-unit-length resistance R increases as the square root of the frequency, and the per-unit-length conductance G increases linearly with frequency. The effect of G can no longer be ignored in the high-frequency range. G is related to the per-unit-length capacitance C as

$$G = \omega \tan(\theta) C \quad (28)$$

First, Z_{ino} is calculated when $\tan(\theta)$ or G is assumed to be zero, and the errors between the calculation and measurement can be observed. Then the exact value of $\tan(\theta)$ or G can be determined to eliminate the errors.

C. METHOD FOR SOLVING PER-UNIT-LENGTH PARAMETERS

By measuring S parameters, the impedance and transmission characteristics of the uniform power line can be obtained [17]. In order to measure the input impedance of CM, the core wires 1 and 3 are connected together at the source end, then the port 1 of network analyzer is connected between core wires 1(or 3) and 2, and the load end of the cable is open. According to the measured S_{11} , the input impedance is

$$Z_{inm} = 50 \frac{1 + S_{11}}{1 - S_{11}} \quad (29)$$

When calculating the input impedance base on the MTL equations, the terminal condition at the source end is

$$\mathbf{I}_C(0) = \mathbf{I}_s - \mathbf{Y}_s \mathbf{U}(0) = \begin{bmatrix} 1 \\ 1 \end{bmatrix} - \begin{bmatrix} 1/50 & 0 \\ 0 & 1/50 \end{bmatrix} \mathbf{U}(0) \quad (30)$$

where the two elements of \mathbf{I}_s should be equal, which are set to 1. According to (5), the terminal voltages and currents can be calculated, and the input impedance of CM can be further calculated.

In order to measure input impedance of DM, the port 1 of network analyzer is connected between core wires 1 and 3, and the core wire 2 is left open. The terminal condition at the source end is

$$\mathbf{I}_D(0) = \mathbf{I}_s - \mathbf{Y}_s \mathbf{U}(0) = \begin{bmatrix} 1 \\ -1 \end{bmatrix} - \begin{bmatrix} 1/50 & -1/50 \\ -1/50 & 1/50 \end{bmatrix} \mathbf{U}(0) \quad (31)$$

The magnitude and phase of input impedances of 40m cable in mode domain are shown in Fig. 3. The results of calculation and measurement have good coherence by comparing, which shows that a simple linear correction can provide sufficient accuracy, thereby avoiding the complex non-linear methods. In this example, the correction coefficients of DM capacitance are $m = 1.08$ and $n = -0.025$, and the correction coefficients of CM capacitance are $m = 0.84$ and $n = -0.025$. $\tan(\theta)$ is 0.05 for both DM and CM.

IV. VALIDATION OF THE MODEL

A. DM AND CM S_{21} FOR 40m CABLE

To verify the accuracy of the model, the transmission characteristics of the 40m cable are calculated based on the model

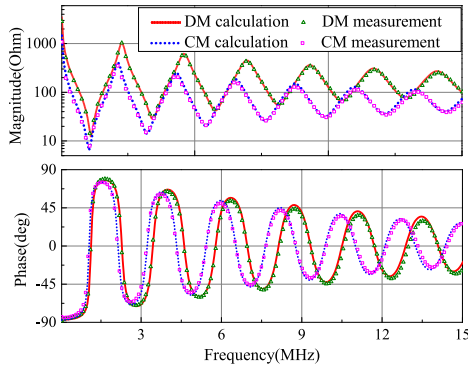


FIGURE 3. Open-circuit impedance of 40m cable.

parameters, and the vector network analyzer is used for measurement. For CM, the load end is equivalent to

$$Y_{CL} = \begin{bmatrix} 1/50 & 0 \\ 0 & 1/50 \end{bmatrix} \quad (32)$$

For DM, the load end is equivalent to

$$Y_{DL} = \begin{bmatrix} 1/50 & -1/50 \\ -1/50 & 1/50 \end{bmatrix} \quad (33)$$

According to (5), S_{21} can be further calculated as

$$S_{21} = \frac{I_l}{0.5I_s} \quad (34)$$

The I_l and I_s are taken from the actual ports where the vector network analyzer is connected.

The magnitude and phase of S_{21} are shown in Fig. 4, which shows that the calculation and measurement are in good agreement. The maximum error of magnitude is not more than 0.8 dB.

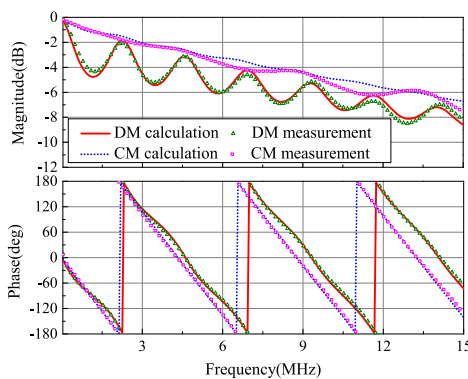


FIGURE 4. S_{21} of 40m cable.

B. INPUT IMPEDANCE OF TEST NETWORK

In order to further verify the accuracy of the model, a T-type network is built as shown in Fig. 5, where the branch cable is 10m.

The input impedance between core wires 1 and 3 of node A is shown in Fig. 6, where node B and C are left open.

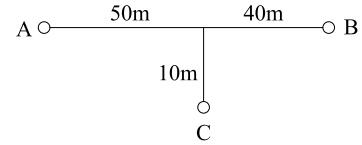


FIGURE 5. Topology of the test network.

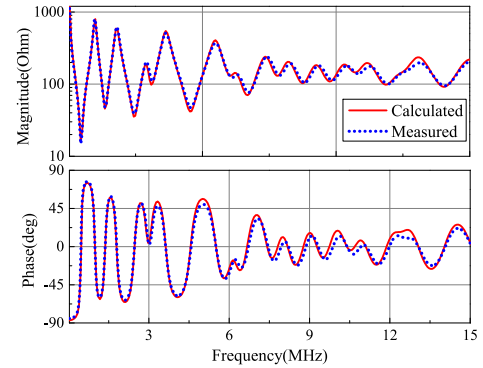


FIGURE 6. Input impedance between 1 and 3 of node A.

The calculation results of magnitude and phase agree well with the measurement results. The measured magnitude varies from 15 to 1122 Ω , and the phase angle is generally not equal to zero. The input impedance between core wires 1 and 2 of node A is shown in Fig. 7. The results are in good agreement also.

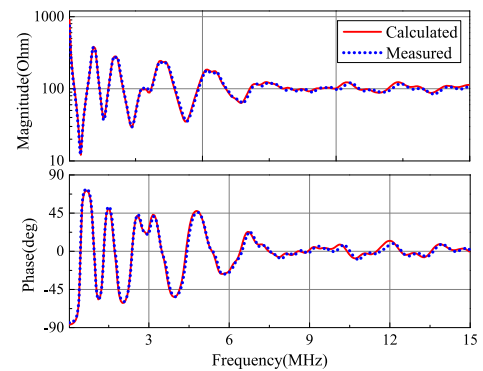


FIGURE 7. Input impedance between 1 and 2 of node A.

C. S_{21} OF TEST NETWORK

To measure S_{21} of test network when the node C is left open, the port 1 of network analyzer is connected to the core wires 1 and 3 of node A, and the port 2 of network analyzer is connected to the core wires 1 and 3 of node B. Fig. 8 compares the calculated and measured S_{21} , which shows good agreement.

In order to further validate the proposed model, the port 1 of network analyzer is connected to core wires 1 and 2 of node A, and the port 2 is connected to core wires 1 and 2 of node B. As shown in Fig. 9, the calculated and measured results match closely. There is relatively small discrepancy in the frequency range above 10 MHz.

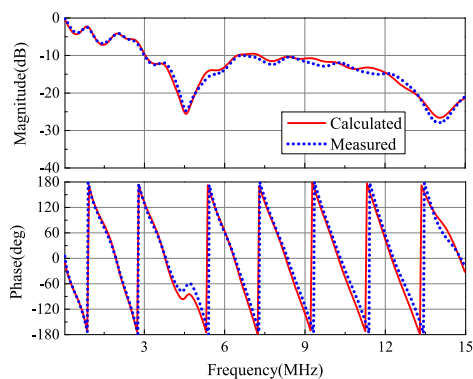


FIGURE 8. S_{21} from 1-3 to 1-3.

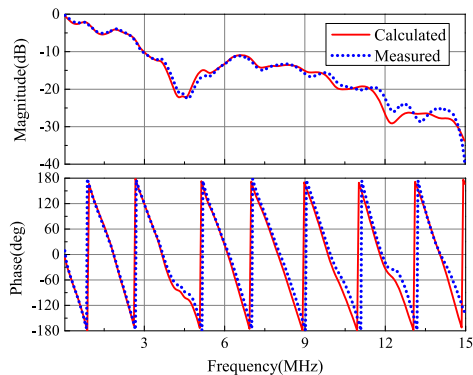


FIGURE 9. S_{21} from 1-2 to 1-2.

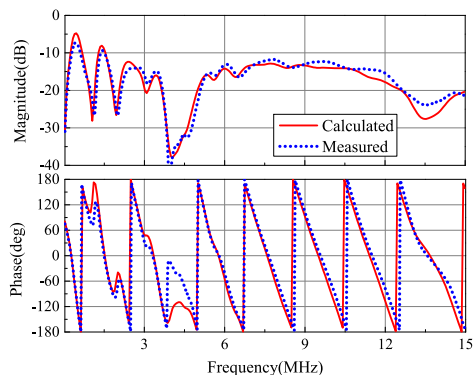


FIGURE 10. S_{21} from 1-2 to 3-2.

Comparing Fig. 8 and Fig. 9, we can see that each magnitude of S_{21} has a deep fading at about 4.5 MHz, which is caused by the input impedance of branch line. When the input impedance of branch line has a valley value, the magnitude of S_{21} has a deep fading.

Based on the MTL method, the coupling effect between core wires can be accurately predicted, which is useful in the design and analysis of MIMO communication system. The next configuration is the coupled channel that the port 1 of network analyzer is connected to core wires 1 and 2 of node A, and the port 2 is connected to core wires 3 and 2 of node B. The results are shown in Fig. 10. The calculated

and measured results are in good agreement except for the frequency near 4 MHz. Compared with the S_{21} of direct channel in Fig. 9, the attenuation of the coupled channel is smaller in the frequency range above 9 MHz. When designing a MIMO communication system, the direct and coupled channels should be fully used for better data rates.

V. CONCLUSION

This paper presents the broadband impedance and transmission model of low-voltage three-core cables. Based on the phase-mode transformation method, the per-unit-length parameter matrices is decomposed into CM and DM parameters. Based on the electromagnetic simulation of the finite element method, the open-circuit impedances of the two modes are measured, and the per-unit-length parameters are linearly corrected to finally obtain the exact values. The accuracy of the channel model is verified by the test network with branch line, and the influence of branch line on channel transmission characteristics is analyzed. The modeling methods which combine simulation and auxiliary measurement have the advantages of accuracy, simplicity and wide application. The establishment of precise cable model can provide a solid foundation for the research of MIMO PLC.

REFERENCES

- [1] P. Pagani and A. Schwager, "A statistical model of the in-home MIMO PLC channel based on European field measurements," *IEEE J. Sel. Areas Commun.*, vol. 34, no. 7, pp. 2033–2044, Jul. 2016.
- [2] A. Schwager, D. Schneider, W. Bäschlin, A. Dilly, and J. Speidel, "MIMO PLC: Theory, measurements and system setup," in *Proc. IEEE Int. Symp. Power Line Commun. Appl. (ISPLC)*, Apr. 2011, pp. 48–53.
- [3] K. Khalil, M. G. Gazelet, P. Corlay, F. X. Coudoux, and M. Gharbi, "An MIMO random channel generator for indoor power-line communication," *IEEE Trans. Power Del.*, vol. 29, no. 4, pp. 1561–1568, Aug. 2014.
- [4] W. B. Cao, C. Q. Yin, Z. Y. Xie, X. L. Liang, and X. C. Li, "Research on broadband MIMO power line communications model," *Proc. CSEE*, vol. 37, no. 4, pp. 1136–1141, Feb. 2017.
- [5] F. Versolatto and A. M. Tonello, "An MTL theory approach for the simulation of MIMO power-line communication channels," *IEEE Trans. Power Del.*, vol. 26, no. 3, pp. 1710–1717, Jul. 2011.
- [6] H. Meng, S. Chen, Y. L. Guan, C. L. Law, P. L. So, E. Gunawan, and T. T. Lie, "Modeling of transfer characteristics for the broadband power line communication channel," *IEEE Trans. Power Del.*, vol. 19, no. 3, pp. 1057–1064, Jul. 2004.
- [7] P. Wagenaars, P. A. A. F. Wouters, P. C. J. M. Van Der Wielen, and E. F. Steennis, "Approximation of transmission line parameters of single-core and three-core XLPE cables," *IEEE Trans. Dielectr. Electr. Insul.*, vol. 17, no. 1, pp. 106–115, Feb. 2010.
- [8] Z. Hasirci, I. H. Cavdar, and M. Ozturk, "Applicability comparison of transmission line parameter extraction methods for busbar distribution systems," *J. Elect. Eng. Technol.*, vol. 12, no. 2, pp. 586–593, Mar. 2017.
- [9] Z. Hasirci, I. H. Cavdar, and M. Öztürk, "RLGC(f) modeling of a busbar distribution system via measured S-parameters at CENELEC and FCC bands," *Turk. J. Elec. Eng. Comp. Sci.*, vol. 26, no. 1, pp. 489–500, 2018.
- [10] J. A. Corchado, J. A. Cortés, F. J. Cañete, and L. Díez, "An MTL-based channel model for indoor broadband MIMO power line communications," *IEEE J. Sel. Areas Commun.*, vol. 34, no. 7, pp. 2045–2055, Jul. 2016.
- [11] Y. H. Guo, Z. Y. Xie, and X. C. Shi, "Modeling of medium voltage power line communication channel based on multi-conductor lines," *Proc. CSEE*, vol. 34, no. 7, pp. 1183–1190, Mar. 2014.
- [12] C. R. Paul, *Analysis of Multiconductor Transmission Lines*. Hoboken, NJ, USA: Wiley, 2007.
- [13] G. Z. Lu, Q. X. Guo, and D. D. Zeng, "Proximity effect and the distribution parameters of multi-conductor transmission line," *Chin. J. Radio Sci.*, vol. 31, no. 3, pp. 611–615, Jun. 2016.

- [14] S. Tsuzuki, T. Takamatsu, H. Nishio, and Y. Yamada, "An estimation method of the transfer function of indoor power-line channels for Japanese houses," in *Proc. IEEE Int. Symp. Power Line Commun. Appl. (ISPLC)*, Mar. 2002, pp. 55–59.
- [15] B. Kruizinga, P. A. A. F. Wouters, and E. F. Steennis, "High frequency modeling of a shielded four-core low voltage underground power cable," *IEEE Trans. Dielectr. Electr. Insul.*, vol. 22, no. 2, pp. 649–656, Apr. 2015.
- [16] A. W. Cirino, H. de Paula, R. C. Mesquita, and E. Saraiva, "Cable parameter variation due to skin and proximity effects: Determination by means of finite element analysis," in *Proc. 35th Annu. Conf. IEEE Ind. Electron.*, Porto, Portugal, Nov. 2009, pp. 4073–4079.
- [17] E. Takmaz, "Impedance, attenuation and noise measurements for power line communication," in *Proc. 4th Int. Istanbul Smart Grid Congr. Fair (ICSG)*, Istanbul, Turkey, Apr. 2016, pp. 1–4.



YIHE GUO was born in Hebei, China, in 1979. He received the B.S. degree in telecommunication engineering from North China Electric Power University, Baoding, China, in 2002, the M.S. degree in information and communication engineering from Beijing Jiaotong University, Beijing, China, in 2005, and the Ph.D. degree in electrical engineering from North China Electric Power University, in 2014. He is currently with North China Electric Power University. His research interests include power line communication and distribution automation.



ZHE YANG was born in Hubei, China, in April 1994. He received the B.S. degree in electronic information science and technology from North China Electric Power University, Baoding, China, in 2016, where he is currently pursuing the M.S. degree in information and communication engineering. His research interests include power line communication and distribution automation.



RAN HUO was born in Hebei, China, in March 1992. She received the B.S. degree in electronic information science and technology from the College of Science and Technology, North China Electric Power University, Baoding, China, in 2015, and the M.S. degree in electronics and communication engineering from North China Electric Power University, in 2019. She is currently a Staff with State Grid Information and Telecommunication Group Company Ltd., Beijing, China. Her research interest includes power line communication.



ZHIYUAN XIE was born in Hebei, China, in May 1964. He received the B.S. degree in telecommunication engineering from North China Electric Power University, Baoding, China, in 1985, the M.S. degree in telecommunication engineering from North China Electric Power University, Beijing, China, in 1994, and the Ph.D. degree in electrical engineering from North China Electric Power University, Baoding, in 2009. He is currently a Professor with the School of Electrical and Electronic Engineering, North China Electric Power University, Baoding. His research interests include power line communication and distribution automation.

...